Title	Cancer-associated fibroblasts regulate tumor-initiating cell plasticity in hepatocellular carcinoma through c-Met/FRA1/HEY1 signaling
Author(s)	Lau, YT; Lo, J; CHENG, YLB; MA, KF; Lee, MF; Ng, KY; CHAI, S; Lin, C; Tsang, FS; Ma, SKY; Ng, IOL; Lee, KW
Citation	Cell Reports, 2016, v. 15 n. 6, p. 1175-1189
Issued Date	2016
URL	http://hdl.handle.net/10722/228967
Rights	This work is licensed under a Creative Commons Attribution-NonCommercial-NoDerivatives 4.0 International License.

Article

Cell Reports

Cancer-Associated Fibroblasts Regulate Tumor-Initiating Cell Plasticity in Hepatocellular Carcinoma through c-Met/FRA1/HEY1 Signaling

Graphical Abstract

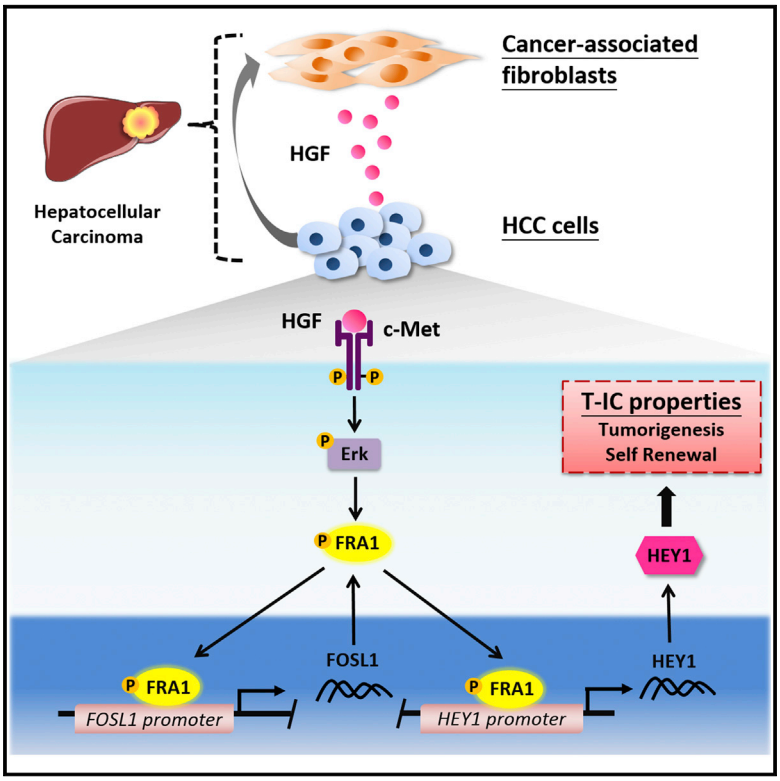

Authors

Eunice Yuen Ting Lau, Jessica Lo, Bowie Yik Ling Cheng, ..., Stephanie Ma, Irene Oi Lin Ng, Terence Kin Wah Lee

Correspondence

iolng@hku.hk (I.O.L.N.), terence.kw.lee@polyu.edu.hk (T.K.W.L.)

In Brief

Similar to normal stem cells, tumor-initiating cells are regulated extrinsically within their microenvironment. Lau et al. find that cancer-associated fibroblasts play a crucial role in the regulation of liver T-ICs through HGF-mediated activation of the c-Met/FRA1/HEY1 cascade. Targeting this pathway may be a promising approach for cancer treatment.

Highlights

- The presence of α-SMA(+) CAFs correlates with poor prognosis of HCC
- CAFs regulate liver T-ICs through paracrine secretion of HGF
- FRA1 is required for HGF/c-Met-mediated T-IC phenotypes
- The HGF-mediated c-Met/FRA1/HEY1 cascade represents a therapeutic target for HCC

Accession Numbers

GSE67927
GSE68005

Lau et al., 2016, Cell Reports *15*, 1175–1189
May 10, 2016
http://dx.doi.org/10.1016/j.celrep.2016.04.019

Cell Reports
Article

OPEN ACCESS
CellPress

Cancer-Associated Fibroblasts Regulate Tumor-Initiating Cell Plasticity in Hepatocellular Carcinoma through c-Met/FRA1/HEY1 Signaling

Eunice Yuen Ting Lau,[1,2,6] Jessica Lo,[1,2,6] Bowie Yik Ling Cheng,[1,2] Mark Kin Fai Ma,[1,2] Joyce Man Fong Lee,[1,2] Johnson Kai Yu Ng,[1,3] Stella Chai,[1,3] Chi Ho Lin,[4] Suk Ying Tsang,[5] Stephanie Ma,[1,3] Irene Oi Lin Ng,[1,2,*] and Terence Kin Wah Lee[1,2,6,*]

[1]State Key Laboratory for Liver Research
[2]Department of Pathology
[3]School of Biomedical Sciences
[4]Centre for Genomic Sciences, Li Ka Shing Faculty of Medicine
The University of Hong Kong, Hong Kong, PRC
[5]School of Life Sciences, The Chinese University of Hong Kong, Hong Kong, PRC
[6]Present address: Department of Applied Biology and Chemical Technology, The Hong Kong Polytechnic University, Hong Kong, PRC
*Correspondence: iolng@hku.hk (I.O.L.N.), terence.kw.lee@polyu.edu.hk (T.K.W.L.)
http://dx.doi.org/10.1016/j.celrep.2016.04.019

SUMMARY

Like normal stem cells, tumor-initiating cells (T-ICs) are regulated extrinsically within the tumor microenvironment. Because HCC develops primarily in the context of cirrhosis, in which there is an enrichment of activated fibroblasts, we hypothesized that cancer-associated fibroblasts (CAFs) would regulate liver T-ICs. We found that the presence of α-SMA(+) CAFs correlates with poor clinical outcome. CAF-derived HGF regulates liver T-ICs via activation of FRA1 in an Erk1,2-dependent manner. Further functional analysis identifies HEY1 as a direct downstream effector of FRA1. Using the STAM NASH-HCC mouse model, we find that HGF-induced FRA1 activation is associated with the fibrosis-dependent development of HCC. Thus, targeting the CAF-derived, HGF-mediated c-Met/FRA1/HEY1 cascade may be a therapeutic strategy for the treatment of HCC.

INTRODUCTION

Hepatocellular carcinoma (HCC) is one of the most common and deadliest malignancies worldwide. The poor prognosis of HCC is attributed to its resistance to chemotherapy and its high rate of recurrence. Increasing evidence shows that tumor-initiating cells (T-ICs), which are capable of tumor initiation, self-renewal, differentiation, and chemoresistance, are responsible for treatment failure and tumor relapse. In HCC, several liver T-IC markers have been identified, including CD13, CD24, CD44, CD47, CD90, CD133, and the epithelial cell adhesion molecule (Haraguchi et al., 2010; Lee et al., 2011, 2014; Yang et al., 2008b; Ma et al., 2007; Yamashita et al., 2009). However, the regulation of liver T-ICs within the tumor microenvironment remains unclear. T-ICs are regulated by both intrinsic and extrinsic signals (Ma et al., 2007; Korkaya et al., 2011) that are generated by the tumor microenvironment. Therefore, a better understanding of how the properties of liver T-ICs are regulated by the tumor microenvironment could lead to the development of a novel therapeutic strategy for targeting liver T-ICs.

Tumor cells are embedded in a complex tumor microenvironment composed of various types of stromal cells, including fibroblasts, inflammatory cells, endothelial cells, and bone marrow-derived cells (Li et al., 2007; Tlsty and Coussens, 2006). Cancer-associated fibroblasts (CAFs) are among the major cell populations within the stromal compartment, and activated fibroblasts are the pre-dominant form of CAFs found in several malignancies. CAFs are best known for their prominent role in tumor development through secretion of tumor-supportive growth factors and nutrients to mediate cancer growth and metastasis (Mazzocca et al., 2010). More than 80% of HCC cases develop within the context of cirrhosis, which is always accompanied by an enrichment of activated fibroblasts due to chronic inflammation (Luedde and Schwabe, 2011). Despite increasing evidence revealing the supportive function of CAFs in HCC, the role of CAFs in regulating liver T-IC properties remains unknown.

To examine the potential role of CAFs in the regulation of liver T-ICs, we isolated, characterized, and propagated CAFs in vitro from fresh HCC clinical samples. We found that CAFs enriched the population of liver T-ICs through paracrine secretion, which could be augmented by the reciprocal interaction between CAFs and HCC cells. Using cytokine profiling, hepatocyte growth factor (HGF) was found to be the most potent mediator of this effect in conditioned medium (CM); this was confirmed by blocking the activation of the HGF/c-Met pathway using an HGF-neutralizing antibody or a c-Met kinase inhibitor. Furthermore, we identified FRA1 as an important mediator of HGF/c-Met-induced T-IC regulation via direct Erk phosphorylation.

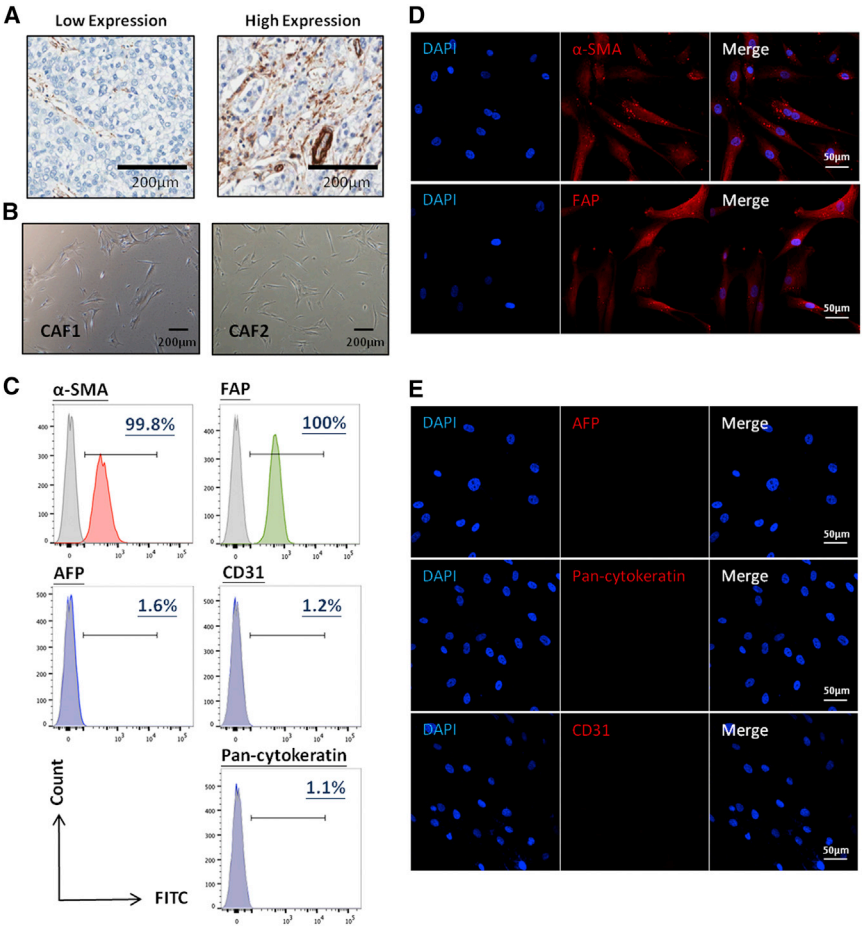

Figure 1. Clinical Significance and Characterization of CAFs Isolated from Freshly Resected HCC Samples

(A) Representative IHC image showing two HCC cases with low α-SMA expression and high α-SMA expression.

(B) Pictures of two batches of CAFs, derived from two HCC specimens, taken under a light microscope. The images show their fibroblast morphology in vitro.

(C–E) As assessed by (C) flow cytometry or (D and E) IF staining, the established CAFs showed (C and D) positive expression for the fibroblast markers α-SMA and FAP and (C and E) negative expression for the epithelial markers pan-cytokeratin and AFP and the endothelial marker CD31.

By using the STAM non-alcoholic steatohepatitis (NASH)-HCC mouse model, we found that HGF-induced FRA1 activation was associated with fibrosis-dependent HCC development. Further RNA sequencing (RNA-seq) analysis identified HEY1, a downstream target of the Notch pathway, as a direct downstream effector of FRA1. FRA1/HEY1 overexpression was significantly correlated with poor patient survival. Our findings may provide an attractive therapeutic approach for targeting the CAF-derived, HGF-mediated c-Met/FRA1/HEY1 cascade to achieve better clinical outcomes for HCC patients.

RESULTS

Isolation, Characterization, and Clinical Significance of CAFs in HCC

CAFs with alpha-smooth muscle actin (α-SMA) expression are considered the main cellular constituents of stroma in a number of cancers (Micke and Ostman, 2005). To understand the role of CAFs in HCC, we evaluated their clinical significance by analyzing the α-SMA expression in 47 HCC patients using immunohistochemical (IHC) staining (Figure 1A). Patients whose tumors had α-SMA overexpression had significantly shorter disease-free survival rates ($p = 0.04$, log rank test). To understand the functional roles of CAFs in HCC, we isolated CAFs from fresh HCC clinical samples. We minced HCC tissues into small pieces and cultured them in vitro, and the culture medium was replenished once every 2 days. After 2–3 weeks of incubation, CAFs that had attached to the culture plate started to grow out; other cell types became unattached and were removed through washing. We then characterized and confirmed the fibroblast identity of the CAFs isolated from the HCC specimens. We found that all CAFs that were established and grew in vitro had a homogenous spindle-shaped fibroblastic morphology (Figure 1B). We analyzed markers of activated fibroblasts, including α-SMA and fibroblast activation protein (FAP), to characterize our established CAFs. We found by flow cytometry analysis that most CAFs displayed positive expression of α-SMA and FAP (Figure 1C). To exclude potential contamination of endothelial cells, HCC cells, and other epithelial cells within the isolated CAF populations, we examined the expression of the respective markers, including CD31, alpha-fetoprotein (AFP), and pan-cytokeratin. Contamination by endothelial cells, HCC cells, and other epithelial these cells in the isolated CAF culture was excluded, as evidenced by ~1% expression of these markers (Figure 1C). This result was confirmed by immunofluorescence (IF) staining, which showed positive staining for α-SMA and FAP and negative staining for CD31, AFP, and pan-cytokeratin (Figures 1D and 1E). Expression of these markers was found to be comparable after several passages (data not shown). Based on these results, all CAFs isolated using this method had a fibroblastic phenotype without contamination of other cell types.

CM of CAFs Regulates Liver T-ICs, an Effect Promoted by the Stimulation of HCC Cells

To determine whether CAFs play a role in regulating tumorigenicity in HCC, we subcutaneously injected HCC cells derived from patient-derived tumor xenograft #1 (PDTX#1) and PDTX#5 into non-obese diabetic/severe combined immunodeficiency

(NOD/SCID) mice alone, with their corresponding CAFs at a ratio of 1:1 or 1:3, or with the CM of CAFs. Compared to the HCC cells injected alone, all groups injected with CAFs or with the CM of CAFs showed greater tumorigenic potential (Figure 2A; Table S1). The effect of CAFs on tumorigenicity was more prominent in HCC cells with CAFs at the ratio of 1:3 when compared with CAFs at the ratio of 1:1. We found that HCC cells injected with CAFs or the CM of CAFs had a similar capacity for enhanced tumorigenicity. These data suggest that CAFs likely perform their regulatory role in cancer mainly through paracrine signaling. Therefore, we collected the CM from CAFs for subsequent in vitro experiments to examine the functional role of the CAFs in regulating the properties of liver T-ICs. To determine whether the CM of CAFs could regulate the self-renewal of HCC cells, Bel-7402 and Huh7 were subjected to a spheroid formation assay with supplementation of either DMEM or CM of normal liver fibroblasts and CAFs. When compared to HCC cells incubated with DMEM and the CM of normal liver fibroblasts, significantly more and larger spheroids were observed in HCC cells incubated with the CM of CAFs (Figure 2B). To confirm the role of CAFs in maintaining self-renewal, we used a pluripotent mouse embryonic stem cell (mESC) line. Under feeder-free conditions, mESCs are maintained as a self-renewing and pluripotent population in the presence of leukemia inhibitory factor (LIF) in the culture medium (Liu et al., 2013). Upon LIF withdrawal, mESCs undergo spontaneous differentiation. We found that the withdrawal of LIF for 48 hr resulted in a decrease in the expression of *Nanog* and *Klf4*, and this effect was reversed in the presence of the CM of CAFs (Figure S1). To investigate whether the CM of CAFs could enrich the T-IC population in HCC cells, we measured by flow cytometry the expression of three liver T-IC markers, CD44, CD47, and CD90, in CM-treated HCC cells (Lee et al., 2014; Yang et al., 2008b). We found that the CM of CAFs enhanced the percentage of populations of these markers in HCC cells (Figure 2C). Specifically, for CD44, we found that CD44s was upregulated in both Bel-7402 and Huh7 cells upon incubation with the CM of CAFs, while CD44v6 was only induced in Bel-7402 cells (data not shown). Using Annexin V/phosphatidylinositol (PI) staining, Huh7 cells and Bel-7402 cells treated with either cisplatin or doxorubicin showed a lower percentage of apoptotic cells when incubated with the CM of CAFs (Figure 2D). Several reports have suggested that T-ICs possess a high metastatic potential (Lee et al., 2011; Yang et al., 2008a). Consistent with these findings, both Bel-7402 and Huh7 cells displayed greater migration and invasion abilities when they were incubated with the CM of CAFs (Figure 2E) and epithelial mesenchymal transition (EMT) was induced (data not shown). Several studies have also demonstrated that tumor cells can educate stromal cells in promoting tumor development (Erez et al., 2010). To examine whether HCC cells educate CAFs to enhance their potential to regulate liver T-ICs, we incubated CAFs with CM collected from Huh7 cells. We found that the CM of educated CAFs (st-CAFs) had a greater ability to promote the self-renewal of HCC cells when compared to the CM of CAFs without education (Figure 2F). This result demonstrated that CAFs could promote liver T-IC properties and, in turn, HCC cells could educate CAFs to increase their potential.

HGF in the CM of CAFs Regulates Liver T-ICs

To identify the key secretory protein in CAF CM that mediates the self-renewal-promoting effect on HCC cells, we compared the cytokine profiles of the CM from Huh7 cells, CAFs, and Huh7-stimulated CAFs by cytokine array (Figure S2A). We found that ten cytokines were identified to be preferentially secreted by CAFs and seven of these were produced upon stimulation by Huh7 cells. These seven factors were interleukin-6 (IL-6), HGF, GCP-2, MCP-1, MCP-2, MCP-3, and RANTES (Figure S2B). The effect of these cytokines on the in vitro self-renewal ability of HCC cells was investigated. Bel-7402 and Huh7 cells were subjected to a spheroid formation assay and supplemented with these seven cytokines at both 10 and 100 ng/ml; HGF was the most potent cytokine in stimulating spheroid formation of HCC cells (Figure S2C). Using ELISA, we found that both CAFs secreted HGF and that this effect was enhanced by stimulation with Huh7 (Figure S2D), confirming the results of the cytokine array profiling. Based on this finding, we turned our attention toward HGF and characterizing its functional role in regulating liver T-ICs. We found that all examined HCC cell lines produced no or negligible levels of HGF, while all CAFs produced a significant amount of HGF, which suggests that CAFs in the tumor stroma are a major source of HGF (Figure 3A). This in vitro finding was confirmed in HCC clinical samples showing a positive correlation between the mRNA expression of *HGF* and the CAF marker *ACTA2* (which encodes for the α-SMA protein) in our HCC clinical samples ($R = 0.7995$, $p < 0.0001$, Pearson correlation) (Figure 3B). To demonstrate that c-Met phosphorylation is due to CAF-derived HGF but not due to HCC itself in an autocrine manner, we first evaluated the activation status of c-Met by assessing phosphorylation at tyrosine residues 1234 and 1235 in a panel of HCC cell lines. Western blotting results showed that in most HCC cell lines, excluding MHCC-97L and MHCC-97H, tyrosine residues 1234 and 1235 of c-Met were not auto-phosphorylated; the phosphorylation event was only observed when these HCC cells were incubated with exogenous HGF (data not shown). To investigate the functional role of CAF-derived HGF in regulating T-ICs, we evaluated the self-renewal ability of T-ICs in vitro by administering recombinant HGF at a level comparable to that secreted by CAFs (2 and 10 ng/ml). At this dosage, we found that HGF resulted in increased c-Met phosphorylation at tyrosine residues 1234 and 1235 in Huh7 and Bel-7402 cells (Figure 3C) and promoted the spheroid formation ability of both cell lines (Figure 3D). We found minimal effect of HGF on spheroid formation of MHCC-97L cells, in which tyrosine residues 1234 and 1235 of c-Met were auto-phosphorylated (data not shown). Using the mESC system described earlier (Figure S1), we found that HGF exerted an effect similar to that of the CM of CAFs, which partially restored the expression of *Nanog* and *Klf4* upon withdrawal of LIF. By Annexin V/PI staining, Huh7 and Bel-7402 cells treated with cisplatin or doxorubicin exhibited decrease in the percentage of the apoptotic population in both cell lines when supplemented with recombinant HGF (Figure 3E). Similar to incubation with the CM of CAFs, we found a significant increase in CD44-, CD47-, or CD90-positive populations after HGF incubation (Figure 3F). In addition, HCC cells displayed increased migration and invasion abilities in the presence of recombinant HGF (Figure 3G). By

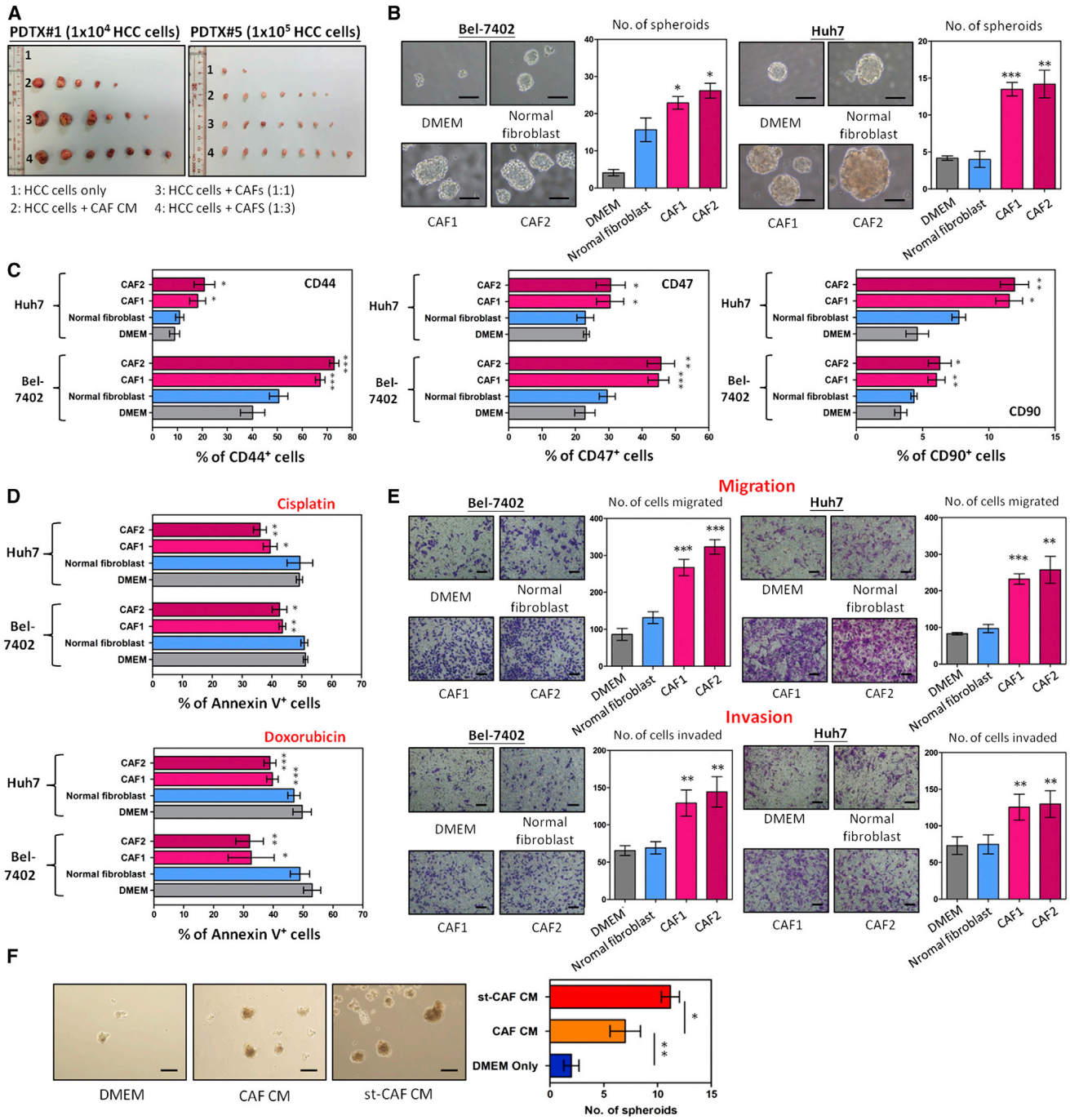

Figure 2. The CM of CAFs Regulates Liver T-ICs

(A) The tumors from PDTX#1 and PDTX#5 were dissociated, and various numbers of tumor cells were subcutaneously injected into the flanks of NOD/SCID mice alone, with CAFs at a 1:1 or 1:3 ratio, or with the CM of CAFs. HCC cells injected with CAFs or the CM of CAFs formed more and larger tumors when compared with HCC cells injected alone.

(B) Bel-7402 cells and Huh7 cells were subjected to a spheroid formation assay supplied with DMEM, the CM of normal liver fibroblasts (Normal fibroblast), or the CM of two batches of CAFs (CAF1 and CAF2). All of them formed significantly more and larger spheroids when supplemented with the CM of CAFs, demonstrating that the CM of CAFs promoted the self-renewal ability of HCC cells.

(C) The CM of CAFs promoted the expression of liver T-IC markers CD44, CD47, and CD90 in HCC cells when compared with the groups incubated with the CM of Normal fibroblast or DMEM only.

(legend continued on next page)

in vivo tumorigenicity assay, we found that HGF-treated Bel-7402 and Huh7 cells exhibited greater tumorigenic ability than did Huh7 cells and Bel-7402 cells alone (Figure 3H; Tables S2A and S2B). Next, we examined whether exogenous HGF preferentially affected liver T-IC populations by comparing the T-IC properties between c-Met$^+$ and c-Met$^-$ populations derived from Huh7 and Bel-7402 cells. We found that c-Met$^+$ enriched liver T-IC populations, as evidenced by an increase in the tumorigenicity and spheroid formation in c-Met$^+$ cells when compared with their negative counterparts (Figures 3I and 3J; Tables S2C and S2D). Finally, we verified the effect of CAF on the regulation of liver T-ICs through secretion of HGF by blocking HGF/c-Met activation using an HGF-neutralizing antibody or the c-Met kinase inhibitor PHA-665752. We found that the inhibition of HGF/c-Met activation using a neutralizing anti-HGF antibody abrogated the effect of CAF CM on the self-renewal, chemoresistance, tumorigenicity, invasiveness, and expression of T-IC markers (Figure S3; Table S3). A similar phenomenon was observed when HCC cells were cultured in the presence of PHA-665752 (Figure S4).

Identification of *FOSL1*/FRA1 as the Downstream Effector of HGF/c-Met-Mediated T-IC Regulation

To delineate the molecular mechanism by which HGF regulates liver T-ICs, we treated Bel-7402 cells with 10 ng/ml of HGF for 18 hr. We then compared the gene expression profile of these cells to that of untreated control cells by cDNA microarray. Upon analysis, we identified a list of genes that were upregulated in response to HGF treatment (Table S4). We focused on FOS-like antigen 1 (*FOSL1*) because it showed an upregulation of 2.7-fold upon HGF treatment. We confirmed the upregulation of the mRNA expression of *FOSL1* and protein expression of FRA1 in Bel-7402 and Huh7 cells following HGF treatment (Figures 4A and 4B). By western blotting, we also demonstrated that the CM of CAFs had a similar effect on FRA1 and this effect was abolished when the CM of CAFs was pre-incubated with either the HGF-neutralizing antibody or the c-Met inhibitor PHA-665752 (Figure 4C), confirming that the effect of CAF on FRA1 was due to the presence of HGF in the CM of CAFs. Next, we examined whether other AP-1 family members would be induced by HGF. By qPCR, we found that the expression of *FOSL1* was the most significantly upregulated member of the AP-1 family, including *FOSB*, *FOSL1*, *FOSL2*, *C-FOS*, *C-JUN*, *JUNB*, and *JUND*, in response to HGF treatment (data not shown), demonstrating that HGF only specifically induced *FOSL1*/FRA1 upregulation in the AP-1 family. Furthermore, we found a positive correlation between the expression of *HGF* and that of *FOSL1* mRNA in HCC clinical samples (n = 55, R = 0.5303, $p < 0.0001$, Pearson correlation) (Figure 4D). We then sought to elucidate the regulatory pathway that mediates HGF-induced FRA1 upregulation by examining Erk1/2, because they are known direct downstream mediators of c-Met (Tsukada et al., 2001). For this purpose, Bel-7402 and Huh7 cells were pre-treated with 10 μM U0126 to block the Erk1/2 pathway and then treated with 10 ng/ml of HGF. The inhibition of Erk1/2 abolished HGF-induced FRA1 phosphorylation and upregulation (Figure 4E). We also found an increase in *FOSL1* mRNA levels in the presence of HGF, and this effect was abolished after the administration of U0126 (Figure 4F). To further understand the molecular mechanism of how *FOSL1* mRNA was upregulated in the presence of HGF, we performed bioinformatics analysis using the University of California Santa Cruz Genome Browser. This analysis found four putative FRA1 binding sites (−15,308, 140, 1,137, and 3,664 bp) near the transcription start site of the *FOSL1* promoter (Figure 4G). Therefore, we hypothesized that *FOSL1* was transcriptionally activated by FRA1 in the presence of HGF. Using a chromatin immunoprecipitation (ChIP)-qPCR assay, we demonstrated the binding between FRA1 and *FOSL1* promoter in Bel-7402 cells (Figure 4G). These data suggested that HGF induces Erk1/2 phosphorylation and subsequent upregulation of FRA1, which leads to the direct transcriptional activation of *FOSL1* in HCC cells to form an auto-feedback loop.

Clinical and Functional Significance of FRA1 in the Regulation of Liver T-ICs

To investigate whether FRA1 was the downstream effector of HGF in regulating liver T-ICs, we successfully knocked down FRA1 (shFRA1-1 and shFRA1-2) in Bel-7402 and Huh7 cells using a lentivirus-based knockdown approach under normal conditions and after HGF treatment (Figure 5A; Figure S5A). Knockdown of FRA1 decreased the number of spheroids formed in both HCC cell lines, indicating that FRA1 is important for self-renewal. In the vector control (shCtl) group, 10 ng/ml of HGF significantly enhanced the spheroid formation ability of HCC cells, as demonstrated in Figure 3D, and this effect was profoundly suppressed upon FRA1 knockdown (Figure 5B; Figure S5B). Next, we demonstrated that HGF-enhanced chemoresistance was mediated by FRA1 (Figure 5C; Figure S5C). To confirm the role of FRA1 in mediating HGF-induced T-IC regulation, we examined the expression of the liver T-IC markers CD44 and CD47 in FRA1 knockdown HCC cells with or without the presence of HGF. FRA1 knockdown not only reduced the expression of CD44 and CD47 but also abolished HGF induced by the expression of both CD44 and CD47 in Bel-7402 and Huh7 cells (Figure 5D; Figure S5D). To verify that FRA1 is essential for

(D) Bel-7402 and Huh7 cells were treated with the chemotherapeutic drugs cisplatin or doxorubicin in the presence of the CM of CAFs, the CM of Normal fibroblast, or DMEM only and evaluated by Annexin V/PI staining. Both Bel-7402 and Huh7 cells exposed to chemotherapeutic drug treatment showed a lower percentage of Annexin V-positive cells in the presence of the CM of CAFs.

(E) Bel-7402 and Huh7 cells were subjected to migration and invasion assays in the presence of the CM of CAFs, the CM of Normal fibroblast, or DMEM only. The CM of CAFs promoted the migration and invasion of both cell lines.

(F) Huh7 cells were subjected to a spheroid formation assay in the presence of DMEM only, CAF CM, or st-CAF CM. CAF CM promoted and st-CAF CM enhanced the number and size of spheroids formed by Huh7 cells.

*$p < 0.05$, **$p < 0.01$, ***$p < 0.001$, Student's t test, CAF1 or CAF2 versus Normal fibroblast. Data are presented as mean ± SD. Scale bars represent 100 μm. See also Figure S1 and Table S1.

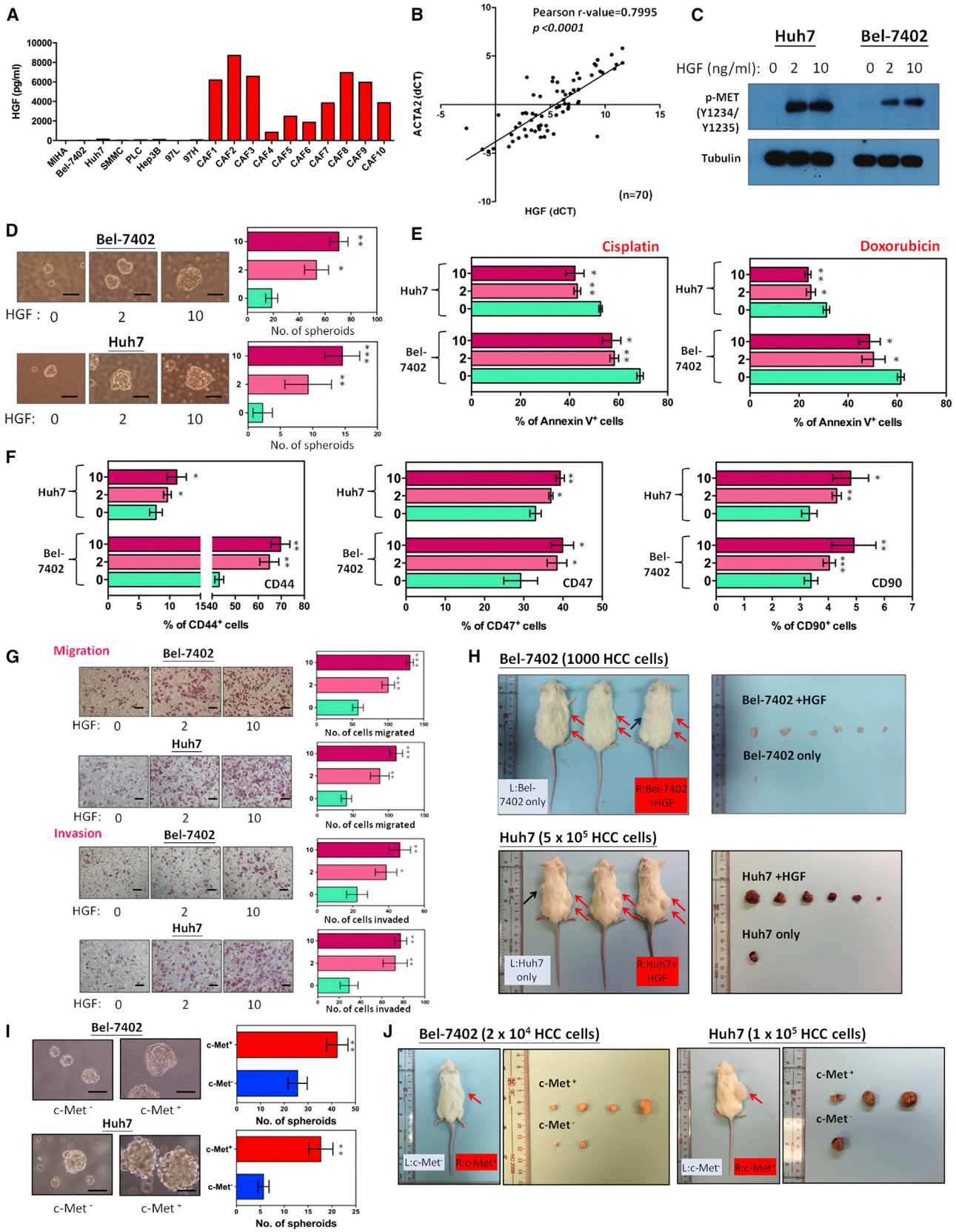

(legend on next page)

the regulation of liver T-ICs, we compared the mRNA expression of *FOSL1* in sorted CD133$^+$ and CD24$^+$ liver T-ICs to that of their negative counterparts. We found that *FOSL1* was preferentially expressed in the CD133$^+$ and CD24$^+$ sub-population when compared to the corresponding CD133$^-$ or CD24$^-$ cells (Figure S5E). In addition, we found the effects of HGF-induced migration and invasion were significantly abolished by FRA1 knockdown (Figure 5E; Figure S5F). Consistent with the preceding in vitro findings, we found that knockdown of FRA1 abolished the tumor enhancing effect of HGF (Figure 5F; Table S5A). Finally, we demonstrated the significance of FRA1 in mediating HGF-induced metastasis using an orthotopic HCC nude mouse model (Figure 5G). Clinically, FRA1 was frequently detected in HCC compared to non-tumor tissue. High FRA1 expression also correlated with reduced disease-free survival ($p = 0.01$, log rank test) and overall survival ($p = 0.029$, log rank test) (Figure 5I).

Stepwise Increase in the Expression of α-SMA, FRA1, T-IC Markers, and Secretory HGF during Fibrosis-Dependent Hepatocarcinogenesis

Because most HCC cases develop in a severe fibrotic or cirrhotic background that is enriched in activated fibroblasts, it would be interesting to investigate whether HGF-dependent FRA1 activation is associated with fibrosis-dependent HCC development. To evaluate the significance of HGF-mediated FRA1 activation in the regulation of liver T-ICs in fibrosis-dependent hepatocarcinogenesis, we employed a STAM NASH-HCC mouse model, in which HCC develops from liver with fibrosis. We obtained the plasma and liver tissues from normal-stage, fibrosis-stage, and HCC-stage mice (Figure 6A). Sirius Red staining confirmed development of HCC in fibrotic background (Figure 6B). Using HGF ELISA, we found stepwise increases in HGF in plasma from the normal stage to the fibrosis stage and the HCC stage (Figure 6C). In addition, cytokines that identified in Figure S2B were found by qPCR analysis to be upregulated in the fibrosis and HCC stages when compared with the normal stage (Figure S6). In parallel with the changes in the plasma HGF levels, we found a similar stepwise increase in the expression of *Acta2, Fosl1* and increases in the liver T-IC markers *Cd44*, *Thy1*, and *Cd24* from the normal to the fibrosis and HCC stages (Figure 6D). By IF staining and confocal microscopy analysis, we found that nuclear staining of FRA1 was absent from normal liver tissue but that FRA1 expression was induced during fibrosis and enhanced in HCC (Figure 6E). These results suggested that activated fibroblasts accumulate during fibrosis, as indicated by *Acta2* upregulation, together with elevated HGF production in the mouse HCC model. We then investigated whether activated fibroblasts in cirrhosis also promoted HCC development through the secretion of HGF in human HCC specimens. To achieve this goal, we extracted non-tumor-associated fibroblasts (NFs) from corresponding non-tumorous liver tissues that were adjacent to HCC but cirrhotic, and we compared the HGF production and self-renewal-promoting abilities of these cells to those of CAFs and normal liver fibroblasts (iBiologics). Consistent with our observations in the mouse model, normal liver fibroblasts secreted only a minimal amount of HGF (400 pg/ml), while CAFs and NFs secreted a significantly greater amount of HGF (3,500–7,000 pg/ml) (Figure 6F). Furthermore, the CM of CAFs and NFs promoted spheroid formation ability in HCC cells, while the CM from normal liver fibroblasts, which did not contain HGF, did not have this effect (Figure 6G). These data verified that activated fibroblasts regulate liver T-ICs through the secretion of HGF.

Identification of HEY1 as the Potential Downstream Effector of FRA1

We subjected FRA1 knockdown (shFRA1-2) Bel-7402 cells and shCtl to RNA-seq in an attempt to search for the transcriptional target of FRA1. In the list of genes that were differentially expressed between the FRA1 knockdown and shCtl groups, we first screened out the genes with a fragments per kilobase of exon per million fragments mapped (FPKM) value of less than 0.01 in the shCtl group and then analyzed the expression of the genes involved in self-renewal pathways, including the

Figure 3. Recombinant HGF Enriches Liver T-IC Populations

(A) CM from a panel of HCC cells and CAFs was collected, and the concentration of HGF was determined using HGF ELISA. All HCC cells secreted no or a very low level of HGF (0–100 pg/ml), while all CAFs secreted a significant amount of HGF (850–8,720 pg/ml).

(B) The qPCR results show positive correlation between *HGF* and *ACTA2* levels ($R = 0.7995$, $p < 0.0001$, Pearson correlation).

(C) Western blot results showing c-Met phosphorylation at tyrosine residues 1234 and 1235 in Huh7 and Bel-7402 cells treated with 2 and 10 ng/ml of HGF.

(D) Bel-7402 and Huh7 cells were subjected to a spheroid formation assay in the presence of 2 or 10 ng/ml of HGF. Both concentrations of HGF enhanced the number and size of spheroids formed compared to the control.

(E) Bel-7402 and Huh7 cells were treated with the chemotherapeutic drugs cisplatin and doxorubicin and 2 or 10 ng/ml of recombinant HGF and were analyzed by Annexin V/PI staining. Bel-7402 and Huh7 cells treated with chemotherapeutic drugs displayed a lower percentage of apoptotic cells in the presence of HGF compared to the DMEM-only control.

(F) The expression of liver T-IC markers CD44, CD47, and CD90 was evaluated by flow cytometry from HCC cells that were untreated or treated with recombinant HGF at 2 or 10 ng/ml for 24 hr. Both concentrations of HGF promoted the expression of liver T-IC markers when compared to the control.

(G) Both concentrations of HGF promoted the migration and invasion of HCC cells, as indicated by an increase in the number of cells that had migrated and invaded through the transwell.

(H) Both Huh7 and Bel-7402 cells were subcutaneously injected into NOD/SCID mice alone or with 10 ng/ml HGF. HCC cells injected with HGF formed more and larger tumors compared to tumor cells injected alone. Black arrows on the left flank represent tumors formed by HCC cells only, while red arrows on the right flank represent tumors formed by HGF-treated cells.

(I) Sorted c-Met$^+$ and c-Met$^-$ HCC cells from Huh7 and Bel-7402 were subjected to spheroid formation assay. The c-Met$^+$ HCC cells formed larger and more spheroids when compared with their c-Met$^-$ counterparts.

(J) Sorted c-Met$^+$ and c-Met$^-$ HCC cells from Huh7 and Bel-7402 were subcutaneously injected into NOD/SCID mice. The c-Met$^+$ HCC cells (right flank, tumors indicated by red arrows) formed more and larger tumors compared with their c-Met$^-$ counterparts (left flank).

*$p < 0.05$, **$p < 0.01$, ***$p < 0.001$, Student's t test. Data are presented as mean ± SD. Scale bars represent 100 μm. See also Figures S2–S4 and Tables S2 and S3.

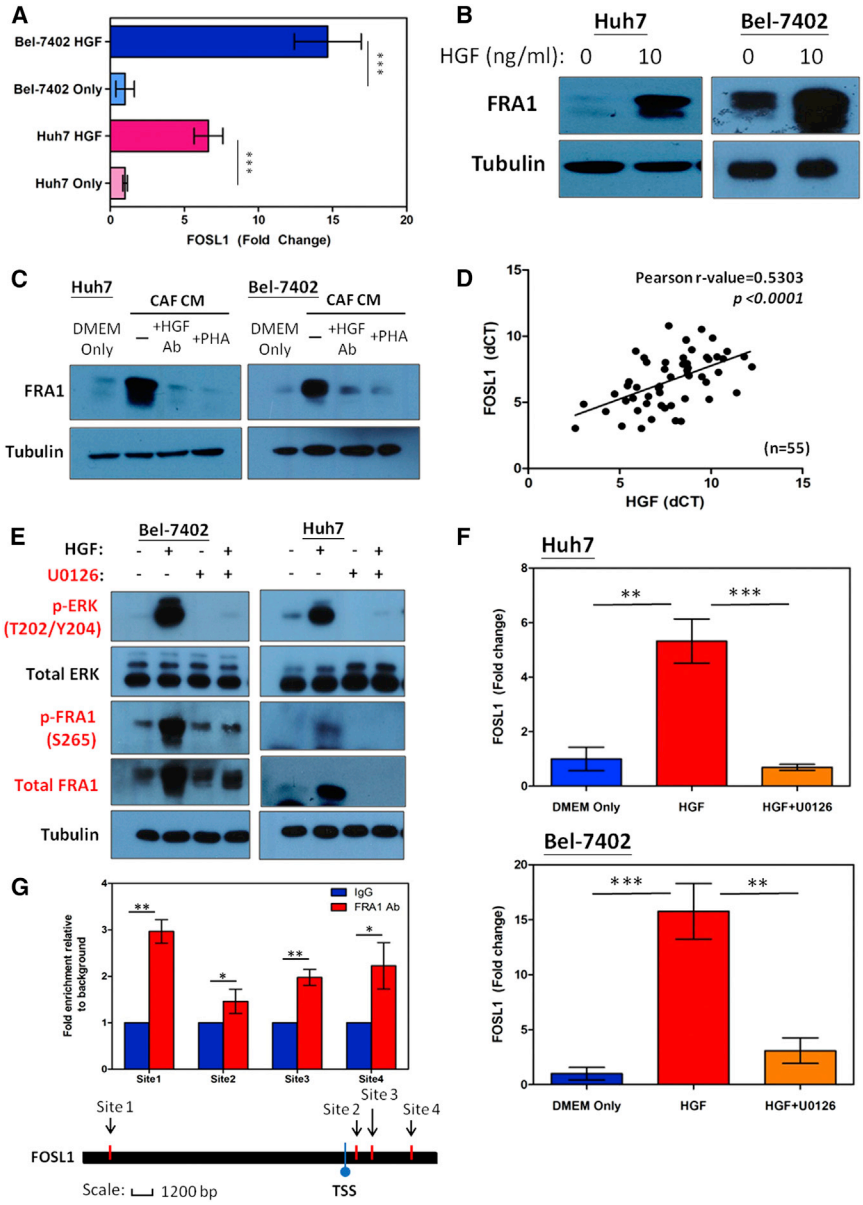

Figure 4. HGF Upregulates FRA1 at Both the mRNA and Protein Levels

(A) HGF promoted the expression of *FOSL1* mRNA in HCC cells. The qPCR results show the mRNA expression of *FOSL1* in Bel-7402 and Huh7 cells in response to 10 ng/ml of HGF treatment for 5 hr. The expression of *FOSL1* increased 14.6-fold in Bel-7402 cells and 6.6-fold in Huh7 cells following HGF treatment. The data are presented as the fold change relative to the untreated group.

(B) HGF and CAF CM increased the expression of the FRA1 protein in HCC cells.

(C) The effect of CAF-induced FRAl expression was abolished by pre-incubation with an HGF-neutralizing antibody or by the addition of the c-Met inhibitor PHA-665752 (PHA). α-Tubulin was used as a loading control.

(D) The qPCR analysis showing the relative mRNA expression of HGF and *FOSL1* in a cohort of 55 HCC clinical samples. The expression levels of HGF and *FOSL1* were positively correlated (R = 0.5303, $p < 0.0001$, Pearson correlation).

(E) Bel-7402 and Huh7 cells were pre-treated with U0126 to inhibit Erk1/2, followed by the administration of 10 ng/ml of HGF. The administration of HGF alone promoted both FRA1 activation and FRA1 expression in HCC cells. Inhibition of Erk1/2 abolished HGF-induced FRA1 activation

(F) The administration of 10 ng/ml HGF increased the expression of FOSL1, and this effect was abolished by the administration of U0126.

(G) FRA1 bound to the *FOSL1* promoter at putative binding sites (site 1, 3.0-fold [$p = 0.005$]; site 2, 1.46-fold [$p = 0.017$]; site 3, 1.98-fold [$p = 0.001$]; and site 4, 2.22-fold [$p = 0.016$]; fold enrichment normalized to IgG control) proximal to the transcriptional start site in Bel-7402 cells.

$^{**}p < 0.01$, $^{***}p < 0.001$, Student's t test. Data are presented as mean ± SD.

Wnt, Shh, Notch, and Hippo pathways, that demonstrated more than 1.5-fold downregulation following FRA1 knockdown (Table S6A). Because we were searching for the direct transcriptional target of FRA1, we excluded genes without a FRA1/AP-1 binding site in their promoter sequence that demonstrated more than 1.5-fold downregulation (Table S6B). By qPCR analysis, we found that *HEY1*, an important downstream effector in the Notch signaling pathway, was the only gene that was consistently downregulated in both FRA1 knockdown clones in both cell lines (Table S6C). Downregulation of HEY1 expression in FRA1 knockdown HCC cells was confirmed (Figure 7A). To evaluate the hypothesis that HEY1 is regulated by FRA1, we transiently overexpressed FRA1 in Bel-7402 and Huh7 cells (Figure S7A). The expression of HEY1 mRNA and protein increased upon FRA1 overexpression (Figures S7B and S7C). To validate the transcriptional regulation of *HEY1* by FRA1, we transfected FRA1 stable knockdown HCC cells with a firefly luciferase construct driven by the *HEY1* promoter and performed a luciferase reporter assay. The firefly luciferase signal was significantly reduced in FRA1 knockdown cells compared to shCtl (Figure 7B). In contrast, the firefly luciferase signal was significantly higher in cells transiently overexpressing FRA1 (Figure S7D), demonstrating that *HEY1* was regulated transcriptionally by FRA1. By ChIP assay, we consistently found binding between FRA1 and the *HEY1* promoter in Bel-7402 cells (Figure 7C). Consistent with the in vitro findings, we observed the co-localization of HEY1 and FRA1 within the nuclei of HCC cells in tissue of HCC clinical samples (Figure 7D). This result was reinforced by the positive correlation between *FOSL1* and *HEY1* expression in a cohort of HCC samples (Figure S7E). To examine whether HEY1 is the downstream effector of FRA1-mediated T-IC regulation, we overexpressed DDK-HEY1 in FRA1 knockdown Bel-7402 cells (Figure 7E). Upon FRA1 knockdown, the number and size of the spheroids formed was greatly reduced,

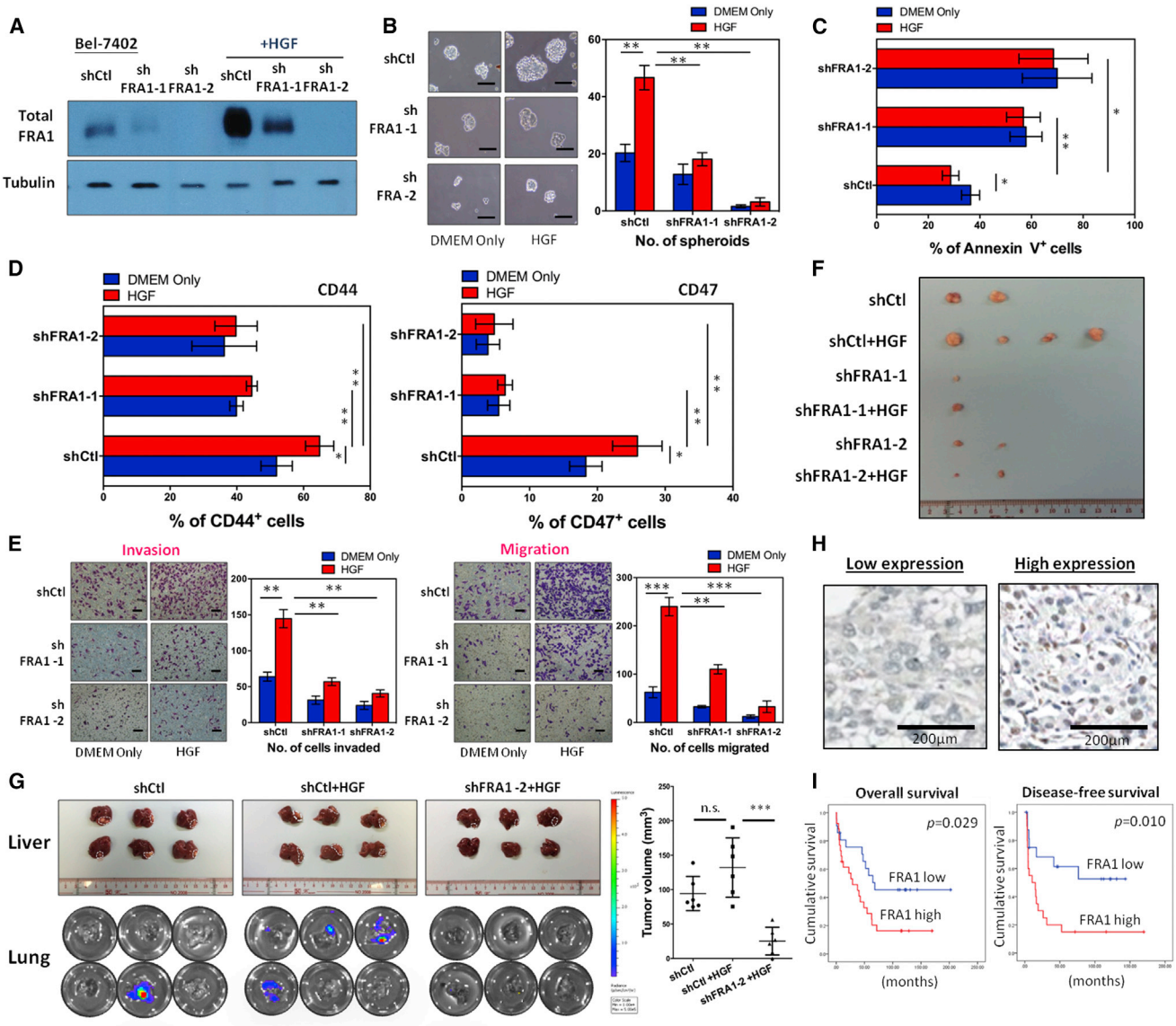

Figure 5. The Effect of FRA1 on HGF-Mediated T-IC Regulation

(A) By western blot, both shFRA1-1 and shFRA1-2 caused a significant reduction of FRA1 expression when compared to shCtl both under normal conditions and in response to HGF treatment.

(B) In the shCtl group, HGF increased both the number and the size of spheroids formed by HCC cells. The effect of HGF-induced spheroid formation was significantly abolished following FRA1 knockdown (shFRA1-1 and shFRA1-2).

(C) FRA1 was knocked down in Bel-7402 cells, and the cells were treated with the chemotherapeutic drug cisplatin in the presence of 10 ng/ml of HGF. Both shFRA1-1 and shFRA1-2 decreased chemoresistance in HCC cells compared to the shCtl. In the shCtl group, HGF enhanced chemoresistance in HCC cells, as indicated by the decreased percentage of Annexin V-positive cells. This effect was abrogated upon FRA1 knockdown.

(D) Both shFRA1-1 and shFRA1-2 decreased the expression of CD44 and CD47 with or without the presence of HGF when compared to shCtl.

(E) Knockdown of FRA1 abolished HGF-induced migration and invasion.

(F) Different numbers of shCtl, shFRA1-1, and shFRA1-2 cells were injected subcutaneously into the flanks of NOD/SCID mice alone or with 10 ng/ml HGF. In the shCtl group, Bel-7402 cells treated with HGF formed more and larger tumors, and this effect was abolished upon FRA1 knockdown.

(G) In an orthotopic HCC metastatic model, HGF induced tumorigenicity and lung metastasis (1/6 versus 4/6) in Bel-7402 cells in vivo, and this effect was abrogated upon FRA1 knockdown (4/6 versus 0/6 for HGF-treated controls and shFRA1 cells). Tumor volume is shown as a dot plot (NS, not significant).

(H) Representative IHC image showing two HCC cases graded with low FRA1 expression and high FRA1 expression.

(I) Kaplan-Meier survival analysis of disease-free survival and overall survival in HCC cases scored as having either low or high FRA1 expression. High FRA1 expression was significantly correlated with shorter disease-free survival ($p = 0.01$, log rank test) and overall survival ($p = 0.029$, log rank test).

*$p < 0.05$, **$p < 0.01$, ***$p < 0.001$, Student's t test. Data are presented as mean ± SD. Scale bars represent 100 μm. See also Figure S5 and Tables S4 and S5.

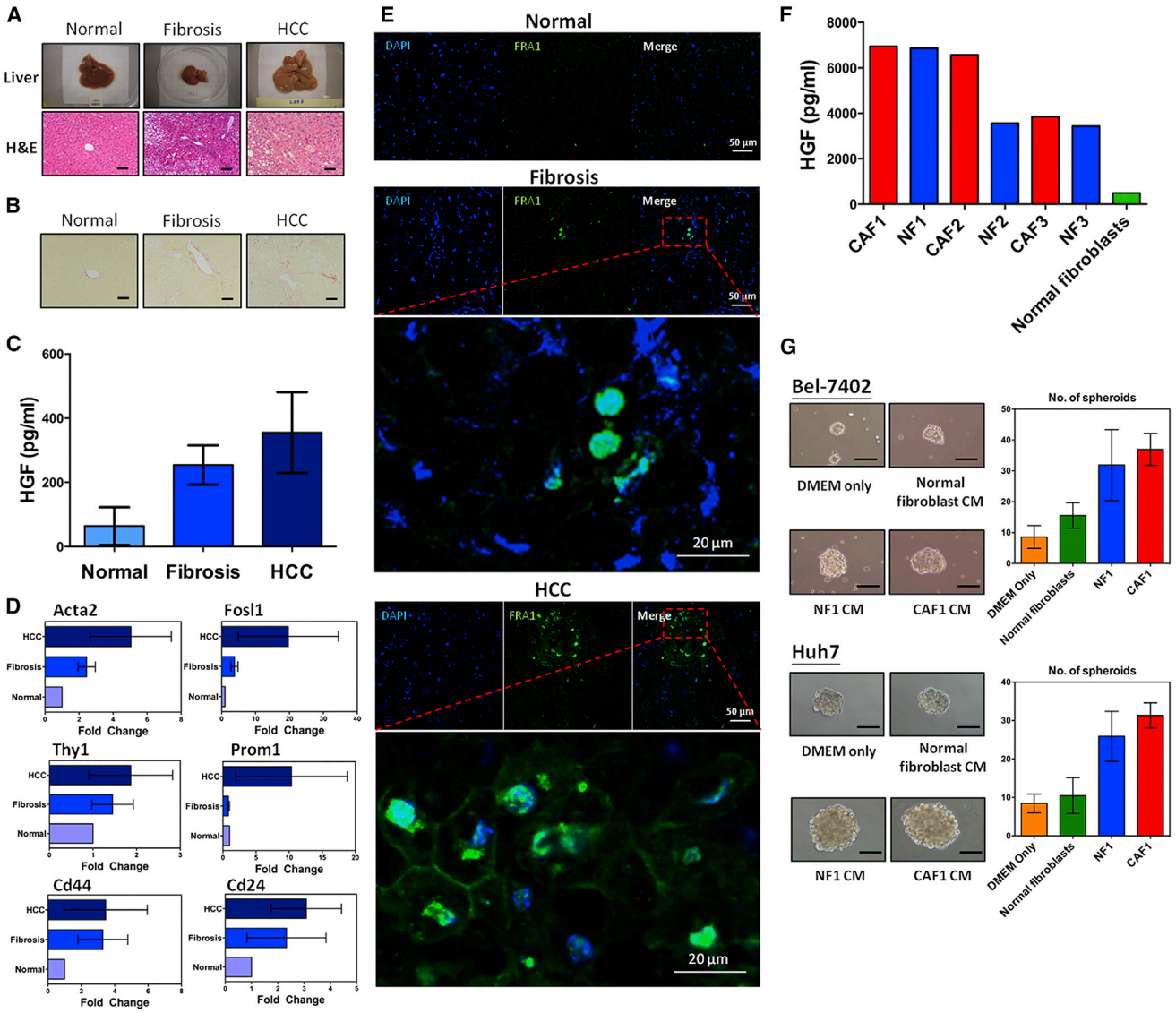

Figure 6. HGF-Dependent FRA1 Activation Is Associated with Fibrosis-Dependent HCC Development

(A) Gross anatomical appearance (upper panel) of the normal-, fibrosis-, and HCC-stage livers from NASH-HCC model mice. The histological appearance (lower panel) at each stage was also analyzed by H&E staining.

(B) Sirius Red staining confirmed the fibrotic background in NASH-HCC model mice.

(C) The level of plasma HGF showed a stepwise increase from normal tissue to fibrotic HCC development (normal = 64 pg/ml versus fibrosis = 250 pg/ml versus HCC = 360 pg/ml). Data show the mean of the plasma HGF concentrations from two mice in the normal stage and three mice each in the fibrosis and HCC stages.

(D) The mRNA expression of the fibroblast marker *Acta2, Fosl1* and liver T-IC markers, including *Cd44*, *Thy1*, *Prom1*, and *Cd24*, in mice from each stage was measured by qPCR.

(E) Frozen sections of the livers from normal-, fibrosis-, and HCC-stage mice in the NASH-HCC mouse model were stained with FRA1 antibody (green) and DAPI (blue) and analyzed by confocal microscopy. A representative confocal image shows FRA1 expression in normal-, fibrosis-, and HCC-stage mice. FRA1 expression was barely detectable during the normal stage. Nuclear staining of FRA1 could be observed in the fibrosis stage but showed the greatest expression in the HCC stage.

(F) The concentrations of HGF in the CM of CAFs (CAF1, CAF2, and CAF3), their paired NFs (NF1, NF2, and NF3), and normal liver fibroblasts were measured using HGF ELISA. CAFs and NFs secreted a significant amount of HGF into the CM (ranging from 3,500 to 7,000 pg/ml), while normal liver fibroblasts secreted only a small amount of HGF into the CM (400 pg/ml).

(G) The CM of CAF1 and NF1 enhanced both the number and the size of the spheroids formed by HCC cells compared to the control (DMEM only) group, while the CM from normal liver fibroblasts was less potent in promoting spheroid formation in HCC cells compared to CAFs and NFs.

Data are presented as mean ± SD. Scale bars represent 100 μm. See also Figure S6.

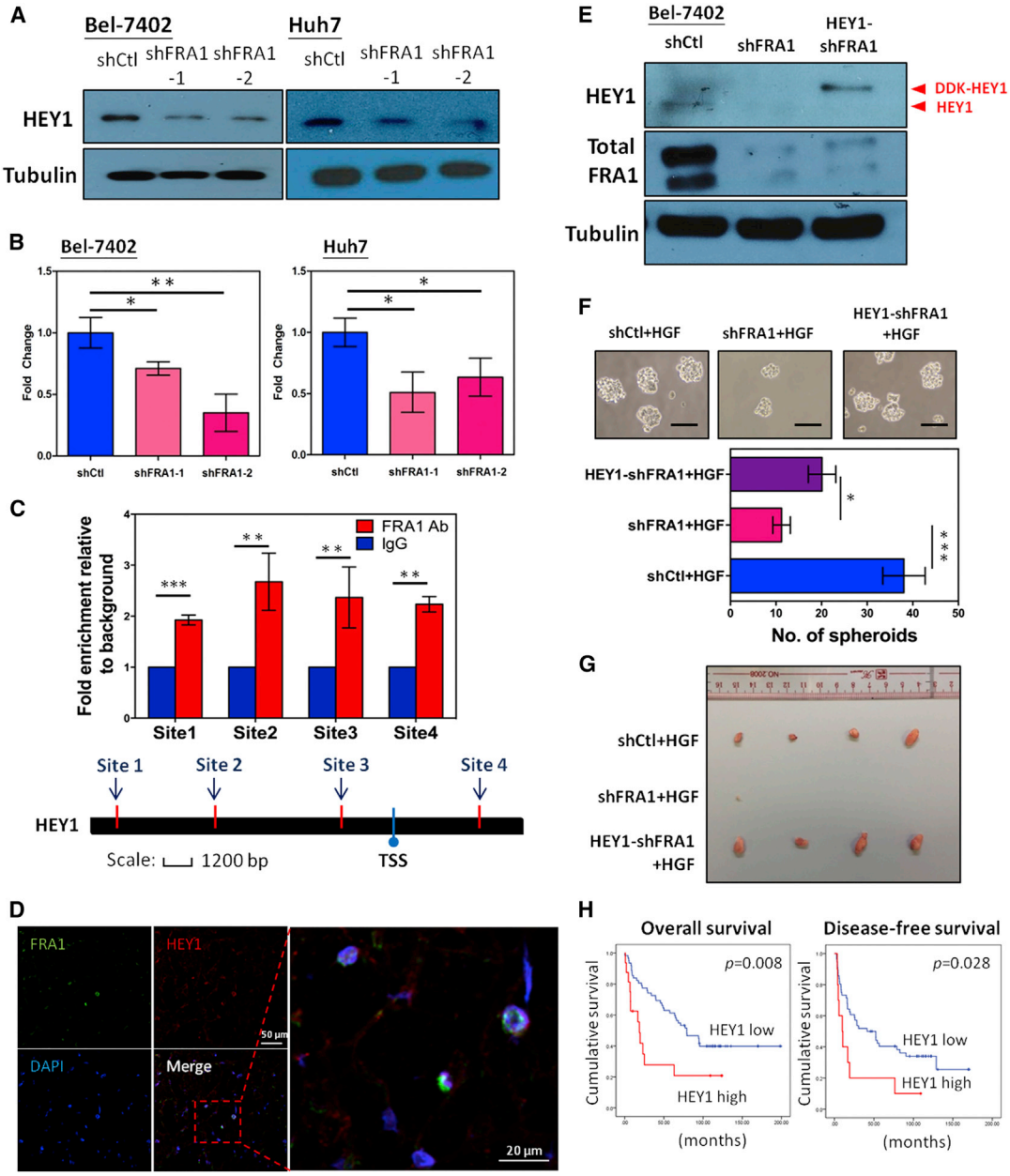

Figure 7. HEY1 Is the Downstream Effector of HGF/c-Met/FRA1 Signaling

(A) The expression of HEY1 was reduced in FRA1 knockdown cells compared to shCtl-treated cells.

(B) The firefly luciferase signal was significantly lower in FRA1 knockdown cells, demonstrating that *HEY1* promoter activity was suppressed following FRA1 knockdown. The data are presented as the fold change relative to the shCtl group.

(C) FRA1 bound to *HEY1* promoter at putative binding sites (site 1, 1.925-fold [p = 0.0003]; site 2, 2.675-fold [p = 0.009]; site 3, 2.367-fold [p = 0.002]; and site 4, 2.233-fold [p = 0.005]; fold enrichment normalized to IgG control) proximal to the transcriptional start site in Bel-7402 cells.

(D) Frozen sections of a human HCC specimen were stained with DAPI (blue), HEY1 antibody (red), and FRA1 antibody (green) and analyzed by confocal microscopy. Co-localization of HEY1 and FRA1 was apparent.

(E) DDK-HEY1 was overexpressed in FRA1 knockdown Bel-7402 cells. Western blot analysis confirmed the overexpression of DDK-HEY1 in FRA1 knockdown Bel-7402 cells, as indicated by the additional band for DDK-HEY1 on top of the endogenous HEY1 protein.

(F) FRA1 knockdown reduced the number and size of the spheroids formed, and this inhibitory effect was partially rescued by HEY1 overexpression.

(G) The shCtl, FRA1 knockdown (shFRA1-2), and HEY1-overexpressing FRA1 knockdown (HEY1-shFRA1) Bel-7402 cells treated with 10 ng/ml of HGF were injected subcutaneously into the flanks of NOD/SCID mice. The inhibitory effect of FRA1 knockdown on tumorigenicity was greatly recovered by HEY1 overexpression.

(H) High *HEY1* expression was significantly correlated with shorter disease-free survival (p = 0.028, log rank test) and overall survival (p = 0.008, log rank test).

*p < 0.05, **p < 0.01, ***p < 0.001, Student's t test. Data are presented as mean ± SD. Scale bars represent 100 μm. See also Figure S7 and Tables S5–S7.

and this inhibitory effect was mostly recovered upon overexpression of HEY1 (Figure 7F). Moreover, we investigated the effect of HEY1 recovery on the tumorigenicity of FRA1 knockdown HCC cells in vivo. We found that the inhibition of tumorigenicity upon FRA1 knockdown was greatly restored by HEY1 overexpression (Figure 7G; Table S5B). Lastly, we retrospectively analyzed the *HEY1* expression in 79 HCC patients by qPCR. The cutoff value of T/N $\geq$ 4 was used to determine *HEY1* expression in HCC patients. Patients whose tumors had high *HEY1* expression were associated with microsatellite formation ($p = 0.044$, chi-square test), and direct liver invasion ($p = 0.007$, Fisher's exact test) (Table S7). Patients whose tumors had *HEY1* overexpression had significantly shorter overall and disease-free survival rates than did those with low *HEY1* expression ($p = 0.008$ and $p = 0.028$, respectively, log rank test).

DISCUSSION

CAFs have been shown to support HCC progression by enhancing tumor cell proliferation and invasiveness (Mazzocca et al., 2010), but the role of CAFs in regulating liver T-IC properties remains unclear. To address this issue, we isolated CAFs from fresh HCC clinical specimens and investigated their functional role in regulating liver T-ICs. CAFs have been shown to be activated fibroblasts in many cancers (Orimo et al., 2005). Several markers that are preferentially expressed by activated fibroblasts, including α-SMA, FAP, desmin, and fibroblast-specific protein, have been widely and commonly used to isolate and identify CAFs in human malignancies. CAFs comprise a heterogeneous population of cells in terms of function and origin (Augsten et al., 2010). However, in our study, we found that 99.8% of the isolated CAFs were α-SMA positive and 100% were FAP positive; these findings demonstrated that the main population of CAFs isolated from HCC consists of activated fibroblasts. To eliminate the possibility of contamination by epithelial cells and endothelial cells, we stained the CAF cultures for the endothelial cell, HCC cell, and epithelial cell markers of CD31, AFP, and pan-cytokeratin, respectively; the CAF culture did not contain any cells expressing these markers. These data demonstrated that we had successfully isolated CAFs from our clinical HCC specimens, established them in an in vitro culture, and characterized their fibroblastic identity. CAFs are known to secrete various types of growth factors, cytokines, and proteases that directly act on tumor cells or other stromal cells to create a tumor-permissive environment. For example, Orimo et al. (2005) showed that CAFs promoted breast tumor growth and angiogenesis through the secretion of SDF-1. In this study, we demonstrated that CAFs, as cellular components within the tumor stroma, exerted a T-IC-promoting effect in HCC through paracrine secretion. However, we uncertain of whether there is an effect when HCC cells are mixed with other cell populations within the tumor stroma, including endothelial cells. Lu et al. (2013) previously demonstrated the role of the CM of endothelial cells in the regulation of T-ICs in colorectal cancer. HCC cells stimulate CAFs to become more potent in promoting the self-renewal of liver T-ICs. Tumor cells are known to actively modify and influence the tumor stroma to create a tumor-supportive niche. It has been reported that cancer cells can secrete several types of growth factors, such as IL-6 or transforming growth factor β1, to activate or stimulate CAFs, leading to their activation and the secretion of tumor-promoting growth factors (Giannoni et al., 2010; Mazzocca et al., 2010).

By cytokine array, we identified HGF as the most prominent CAF-derived cytokine in promoting HCC self-renewal. Aberrant HGF/c-Met activation has been reported in many cancers, including HCC, in which overexpression of HGF has been associated with a poor prognosis (Xie et al., 2013). Using HGF ELISA, we found that HCC cell lines do not secrete HGF, while CAFs secrete a significant amount of HGF. Consistently, we observed that HCC cells do not show auto-activation of c-Met, which could only be activated by the CM of CAFs containing CAF-derived HGF. c-Met is the only receptor of HGF, which was found to be mainly expressed in epithelial cells such as cancer cells (Comoglio et al., 2008). Based on this observation, the effect of CAF-derived HGF on other cell types within the tumor microenvironment is not obvious. The emerging role of the HGF/c-Met pathway in regulating cancer stemness also has been revealed in a few studies. In pancreatic cancer, c-Met was found to be a marker for pancreatic T-ICs, and c-Met^{high} cells readily formed spheroids in vitro. The activation of the HGF/c-Met pathway was found to increase T-IC properties in other cancers by triggering EMT, Wnt signaling, and Notch signaling (Sigurdsson et al., 2011; Vermeulen et al., 2010). By a cell-sorting approach, we found that c-Met^{+} populations enhanced liver T-IC populations, as evidenced by increased abilities in self-renewal and tumorigenicity. In addition, a similar effect in self-renewal was observed in the presence of the CM of CAFs. This result highlights the role of CAF-derived HGF in the regulation of liver T-ICs. We found that physiological levels of recombinant HGF in CAFs enriched liver T-IC populations, as evidenced by an increase in tumorigenicity, self-renewal, chemoresistance, and the expression of T-IC markers. The use of an HGF-neutralizing antibody or the c-Met inhibitor PHA-665752 efficiently neutralized CAF-derived HGF and blocked c-Met activation, thereby abolishing the induction of the HGF/c-Met pathway and the subsequent effect on T-IC properties. This result supports the therapeutic potential of the use of the HGF-neutralizing antibody and c-Met inhibitor for treatment of HCC.

By cDNA microarray profiling analysis, we identified *FOSL1*/FRA1 as a potential downstream effector of HGF. FRA1 is a member of the FOS family (c-FOS, FOSB, FRA1, and FRA2), members of which bind to the JUN-family proteins (c-JUN, JUNB, and JUND) to form the AP-1 transcription factor complex. The divergent and specific functionalities of AP-1 proteins have also been reported. For example, Grigoriadis et al. (1993) showed that transgenic mice overexpressing c-FOS developed osteosarcomas but mice expressing FOSB or c-JUN did not. Such findings suggest that every AP-1 protein has a specific role and that family members are not functionally redundant. In our study, HGF treatment of HCC cells specifically promoted the expression of FRA1 but not other AP-1 family members, indicating that the specific function of FRA1 is required to mediate the effects of HGF in HCC. By western blot analysis, we found that HGF significantly upregulated

FRA1 expression and activated FRA1 by phosphorylation through Erk1/2; this effect was abolished by the administration of an Erk inhibitor. The emerging role of FRA1 in regulating cancer stemness has also been reported in breast cancer (Tam et al., 2013). By generating FRA1 knockdown cells, we confirmed that FRA1 is crucial for mediating the effects of HGF on liver T-IC properties. These in vitro findings were verified by the clinical observation that high FRA1 expression correlated with poorer cellular differentiation in human HCC. In addition, FRA1 overexpression was significantly correlated with poor survivals in HCC patients.

We used the STAM NASH-HCC mouse model to investigate whether FRA1 activation is involved in fibrosis-dependent hepatocarcinogenesis. We found that HGF, the activated fibroblast marker *Acta2, Fosl1*, and liver T-IC markers concurrently increased stepwise from the normal stage to the fibrosis stage and eventually to the HCC stage. This study indicated that the generation and maintenance of stem-like pre-malignant cells are necessary to drive hepatocarcinogenesis. Given the functional significance of FRA1 in promoting liver T-IC properties and its positive association with liver T-IC marker expression in fibrotic hepatocarcinogenesis, HGF-induced FRA1 activation during liver fibrosis may be crucial in supporting the growth of tumor progenitors. We demonstrated that fibroblasts from the fibrotic liver also secrete a significant amount of HGF and promote the self-renewal of HCC cells. Our data provide evidence that FRA1 activation, which is probably induced by the secretion of HGF from activated fibroblasts that accumulate during fibrosis, is associated with fibrosis-dependent hepatocarcinogenesis.

We compared the gene expression profiles of FRA1 knockdown (shFRA1-2) and shCtl Bel-7402 cells by RNA-seq. We showed that HEY1, which contains an AP-1 binding sequence near its promoter sequence, was downregulated at the mRNA and protein levels following FRA1 knockdown in both HCC cell lines. The HEY1 transcription factor is a canonical downstream effector gene in the Notch signaling pathway (Harrison et al., 2010). However, only a few reports have investigated the specific role of HEY1 in regulating these cells. In pancreatic cancer, the expression of *HEY1* was found to be higher in the DCLK1^{HI} T-IC subpopulation than in its more differentiated counterpart (Bailey et al., 2014). In HCC, the ectopic expression of HEY1 promoted HCC tumorigenicity (Jia et al., 2011). The overexpression of HEY1 in FRA1 knockdown cells reversed the reduction in self-renewal and tumorigenesis upon FRA1 knockdown, suggesting that HEY1 is a downstream effector of FRA1 in the regulation of T-ICs. We then demonstrated a direct interaction between FRA1 and *HEY1* by ChIP assays. This in vitro finding was verified in vivo, showing the co-localization of the HEY1 and FRA1 proteins in the nuclei of HCC cells in clinical HCC samples.

In summary, we identified c-Met/FRA1/HEY1 signaling in the CAF-derived, HGF-mediated regulation of liver T-ICs. Our results provide a better understanding of how liver T-ICs are regulated in the tumor microenvironment and reveal a potential target that could be used for the development of more effective therapeutic strategies in HCC. Further investigation of comparing therapeutic inhibition between traditional HGF/c-Met and c-Met/FRA1/HEY1 is awaited.

EXPERIMENTAL PROCEDURES

Patient Samples

Primary HCC and corresponding adjacent non-tumor liver tissues were obtained from patients at Queen Mary Hospital, Pamela Youde Nethersole Eastern Hospital, and Queen Elizabeth Hospital in Hong Kong. All tissue specimens were snap-frozen in liquid nitrogen and stored at −80°C or formalin fixed and paraffin embedded for IHC study. The use of human samples was approved by the Institutional Review Board of the University of Hong Kong and the Hospital Authority Hong Kong.

Cell Lines and Cell Culture

The human HCC cell lines Huh7 and HLE were obtained from the Japanese Cancer Research Bank. Bel-7402, SMMC-7721, and PLC-8024 were obtained from the Shanghai Institutes for Biological Sciences, Chinese Academy of Sciences. Hep3B, SNU-182, and HepG2 were purchased from the American Type Culture Collect (ATCC). MHCC-97L, MHCC-97H, and MHCC-LM3 were provided by Liver Cancer Institute, Fudan University, China. The immortalized normal liver cell line, MIHA, was kindly provided by Dr. J.R. Chowdhury, Albert Einstein College of Medicine, New York. 293FT cells were purchased from Invitrogen. The mESC line D3 was purchased from ATCC. Normal liver fibroblasts were purchased from iBiologics.

Isolation and In Vitro Establishment of CAFs and NFs from Fresh HCC Samples

Fresh HCC samples and their corresponding non-tumor counterparts were washed with serum-free DMEM/F-12 medium and finely minced into small pieces of approximately 0.2 × 0.2 mm. The minced samples were incubated in fresh culture medium for 24 hr to allow attachment to the culture plate. Following incubation, the unattached cells were removed, and the remaining cells were allowed to grow on the plate for 2–3 weeks. In this period, the medium was replenished once every 2 days until the fibroblasts started to grow out. The fibroblasts were checked for >90% positive staining for the fibroblast markers α-SMA and FAP and negative staining for the endothelial cell marker, HCC cell marker, and epithelial cell marker (CD31, AFP, and pan-cytokeratin, respectively) to make sure that there was no contamination of other cell types before the cells were subjected to experiments. The fibroblasts isolated from tumor tissue were defined as CAFs, and those isolated from the non-tumor counterpart were defined as NFs. CAFs and NFs with no more than ten passages were used for experiments.

In Vivo Tumorigenicity Experiments

The study protocol was approved by and performed in accordance with the Committee of the Use of Live Animals in Teaching and Research at The University of Hong Kong. Various numbers of HCC cells resuspended in 50 μl medium mixed with 50 μl Matrigel Matrix (BD Biosciences) were injected subcutaneously into the flanks of NOD/SCID mice. Mice were sacrificed within 5 months post injection, at which time tumors were harvested. T-IC frequency was calculated using the Extreme Limiting Dilution Analysis (ELDA) software (Hu and Smyth, 2009) with 95% CI. For examining the in vivo tumorigenicity of HCC cells derived from PDTXs, HCC cells of various cell numbers alone or together with CAFs at a ratio of 1:1 or 1:3, or with the CM of CAFs were subcutaneously injected into the flanks of NOD/SCID mice as described above. For CM of CAFs groups, the cells were resuspended in 50 μl CAF CM instead of medium, and 50 μl CAF CM was supplemented once every 2 days for a total of 3 rounds by injecting into the site of tumor engraftment.

Collection of CM

CAFs, NFs, normal liver fibroblasts, or HCC cells were seeded on six-well plates at 1 × 10^5 cells per well density. Culture medium was removed 24 hr after cell seeding, cells were washed once with PBS, and 1 ml of serum-free medium was added per well. After 24 hr of incubation at 37°C, the CM was collected and passed through a 0.2 μm membrane syringe filter to remove any cells and cell debris.

For neutralization of HGF in the CM of CAFs, CM was pre-incubated with 10 μg/ml of human HGF antibody or its immunoglobulin G (IgG) control (R&D Systems) for 1 hr at room temperature before it was subjected to experimental use.

Mouse Models

The STAM NASH-HCC mouse model was developed by and purchased from Stelic Institute & Co., and HCC was developed from the NASH background. The liver tissues and plasma from two normal mice of the same strain (C57BL/6J) and 8 weeks of age were acquired from the Animal & Plant Care Facility of the Hong Kong University of Science and Technology to serve as controls.

Patient Sample Processing and Development of PDTX

Fresh HCC samples were dissociated by the gentleMACS dissociator (Miltenyi) in the presence of 20 μg/ml DNaseI (Roche) and 4 μg/ml liberase (Roche). The viability of the cells was evaluated by trypan blue staining (Sigma-Aldrich). Then, 1×10^6 live cells were resuspended, mixed with Matrigel Matrix (BD Biosciences) at a 1:1 ratio, and subcutaneously injected into the flanks of NOD/SCID mice. The tumor developed from the mice was regarded as the PDTX. A number was assigned for each PDTX specific to the patient from whom the tumor was resected.

Statistical Analysis

The statistical significance of the results obtained for the dual-luciferase reporter assay, ChIP-qPCR, qPCR, spheroid formation assay, flow cytometry analysis, invasion and migration assays, and in vivo tumor formation assay was determined by Student's t tests using Microsoft Office Excel software. The results are shown as the means and SDs, and p values of less than 0.05 were considered statistically significant (*$p < 0.05$, **$p < 0.01$, ***$p < 0.001$). Pearson's correlation analysis was used to determine the correlations among *HGF*, *ACTA2, FOSL1*, and *HEY1* expression using Prism 6 software (v.6.04, GraphPad). Pearson's chi-square test and Fisher's exact test were used to assess the correlations between clinicopathological parameters and FRA1 or *HEY1* expression. Kaplan-Meier survival analysis was used to analyze disease-free survival and overall survival, and the statistical significance was calculated by log rank test; these analyses were carried out using SPSS 17.

Additional experimental procedures are provided in the Supplemental Information.

ACCESSION NUMBERS

The accession numbers for both cDNA microarray and RNA-seq data reported in this paper are GenBank: GSE67927 and GSE68005.

SUPPLEMENTAL INFORMATION

Supplemental Information includes Supplemental Experimental Procedures, seven figures, and seven tables and can be found with this article online at http://dx.doi.org/10.1016/j.celrep.2016.04.019.

AUTHOR CONTRIBUTIONS

E.Y.T.L., I.O.L.N., and T.K.W.L. designed the experiment. J.L., B.Y.L.C., M.K.F.M., J.M.F.L., J.K.Y.N., S.C., and S.M. performed the experiment. E.Y.T.L., S.Y.T., and C.H.L. analyzed the data. E.Y.T.L., T.K.W.L., and I.O.L.N. wrote the paper. T.K.W.L. and I.O.L.N. supervised the study. All authors contributed to the discussion of results and manuscript corrections.

ACKNOWLEDGMENTS

The authors thank the LKS Faculty of Medicine at The University of Hong Kong for use of the Faculty Core Facility. The authors also thank Dr. Jiri Zavadil from the Molecular Mechanisms and Biomarkers Group, International Agency for Research on Cancer, Lyon, France, for the pGL3-HEY1 promoter plasmid. The authors thank Dr. Regina Lo for advice on quantitation of FRA1 staining in HCC. The project was supported by the Seed Funding Programme for Basic Research, HKU (201310159034), Hong Kong Research Grants Council General Research Fund (HKU 717111614), Hong Kong Research Grants Council Collaborative Research Fund (C7027-14G), SK Yee Medical Research Fund 2011, and the Lee Shiu Family Foundation. I.O.L.N. is the Loke Yew Professor in Pathology.

Received: May 16, 2015
Revised: January 6, 2016
Accepted: March 31, 2016
Published: April 28, 2016

REFERENCES

Augsten, M., Hägglöf, C., Peña, C., and Ostman, A. (2010). A digest on the role of the tumor microenvironment in gastrointestinal cancers. Cancer Microenviron. *3*, 167–176.

Bailey, J.M., Alsina, J., Rasheed, Z.A., McAllister, F.M., Fu, Y.Y., Plentz, R., Zhang, H., Pasricha, P.J., Bardeesy, N., Matsui, W., et al. (2014). DCLK1 marks a morphologically distinct subpopulation of cells with stem cell properties in preinvasive pancreatic cancer. Gastroenterology *146*, 245–256.

Comoglio, P.M., Giordano, S., and Trusolino, L. (2008). Drug development of MET inhibitors: targeting oncogene addiction and expedience. Nat. Rev. Drug Discov. *7*, 504–516.

Erez, N., Truitt, M., Olson, P., Arron, S.T., and Hanahan, D. (2010). Cancer-associated fibroblasts are activated in incipient neoplasia to orchestrate tumor-promoting inflammation in an NF-kappaB-dependent manner. Cancer Cell *17*, 135–147.

Giannoni, E., Bianchini, F., Masieri, L., Serni, S., Torre, E., Calorini, L., and Chiarugi, P. (2010). Reciprocal activation of prostate cancer cells and cancer-associated fibroblasts stimulates epithelial-mesenchymal transition and cancer stemness. Cancer Res. *70*, 6945–6956.

Grigoriadis, A.E., Schellander, K., Wang, Z.Q., and Wagner, E.F. (1993). Osteoblasts are target cells for transformation in c-fos transgenic mice. J. Cell Biol. *122*, 685–701.

Haraguchi, N., Ishii, H., Mimori, K., Tanaka, F., Ohkuma, M., Kim, H.M., Akita, H., Takiuchi, D., Hatano, H., Nagano, H., et al. (2010). CD13 is a therapeutic target in human liver cancer stem cells. J. Clin. Invest. *120*, 3326–3339.

Harrison, H., Farnie, G., Howell, S.J., Rock, R.E., Stylianou, S., Brennan, K.R., Bundred, N.J., and Clarke, R.B. (2010). Regulation of breast cancer stem cell activity by signaling through the Notch4 receptor. Cancer Res. *70*, 709–718.

Hu, Y., and Smyth, G.K. (2009). ELDA: extreme limiting dilution analysis for comparing depleted and enriched populations in stem cell and other assays. J. Immunol. Methods *347*, 70–78.

Jia, D., Wei, L., Guo, W., Zha, R., Bao, M., Chen, Z., Zhao, Y., Ge, C., Zhao, F., Chen, T., et al. (2011). Genome-wide copy number analyses identified novel cancer genes in hepatocellular carcinoma. Hepatology *54*, 1227–1236.

Korkaya, H., Liu, S., and Wicha, M.S. (2011). Breast cancer stem cells, cytokine networks, and the tumor microenvironment. J. Clin. Invest. *121*, 3804–3809.

Lee, T.K., Castilho, A., Cheung, V.C., Tang, K.H., Ma, S., and Ng, I.O. (2011). CD24(+) liver tumor-initiating cells drive self-renewal and tumor initiation through STAT3-mediated NANOG regulation. Cell Stem Cell *9*, 50–63.

Lee, T.K., Cheung, V.C., Lu, P., Lau, E.Y., Ma, S., Tang, K.H., Tong, M., Lo, J., and Ng, I.O. (2014). Blockade of CD47-mediated cathepsin S/protease-activated receptor 2 signaling provides a therapeutic target for hepatocellular carcinoma. Hepatology *60*, 179–191.

Li, H., Fan, X., and Houghton, J. (2007). Tumor microenvironment: the role of the tumor stroma in cancer. J. Cell. Biochem. *101*, 805–815.

Liu, J.W., Hsu, Y.C., Kao, C.Y., Su, H.L., and Chiu, I.M. (2013). Leukemia inhibitory factor-induced Stat3 signaling suppresses fibroblast growth factor 1-induced Erk1/2 activation to inhibit the downstream differentiation in mouse embryonic stem cells. Stem Cells Dev. *22*, 1190–1197.

Lu, J., Ye, X., Fan, F., Xia, L., Bhattacharya, R., Bellister, S., Tozzi, F., Sceusi, E., Zhou, Y., Tachibana, I., et al. (2013). Endothelial cells promote the colorectal cancer stem cell phenotype through a soluble form of Jagged-1. Cancer Cell *23*, 171–185.

Luedde, T., and Schwabe, R.F. (2011). NF-κB in the liver–linking injury, fibrosis and hepatocellular carcinoma. Nat. Rev. Gastroenterol. Hepatol. *8*, 108–118.

Ma, S., Chan, K.W., Hu, L., Lee, T.K., Wo, J.Y., Ng, I.O., Zheng, B.J., and Guan, X.Y. (2007). Identification and characterization of tumorigenic liver cancer stem/progenitor cells. Gastroenterology *132*, 2542–2556.

Mazzocca, A., Fransvea, E., Dituri, F., Lupo, L., Antonaci, S., and Giannelli, G. (2010). Down-regulation of connective tissue growth factor by inhibition of transforming growth factor beta blocks the tumor-stroma cross-talk and tumor progression in hepatocellular carcinoma. Hepatology *51*, 523–534.

Micke, P., and Ostman, A. (2005). Exploring the tumour environment: cancer-associated fibroblasts as targets in cancer therapy. Expert Opin. Ther. Targets *9*, 1217–1233.

Orimo, A., Gupta, P.B., Sgroi, D.C., Arenzana-Seisdedos, F., Delaunay, T., Naeem, R., Carey, V.J., Richardson, A.L., and Weinberg, R.A. (2005). Stromal fibroblasts present in invasive human breast carcinomas promote tumor growth and angiogenesis through elevated SDF-1/CXCL12 secretion. Cell *121*, 335–348.

Sigurdsson, V., Hilmarsdottir, B., Sigmundsdottir, H., Fridriksdottir, A.J., Ringnér, M., Villadsen, R., Borg, A., Agnarsson, B.A., Petersen, O.W., Magnusson, M.K., and Gudjonsson, T. (2011). Endothelial induced EMT in breast epithelial cells with stem cell properties. PLoS ONE *6*, e23833.

Tam, W.L., Lu, H., Buikhuisen, J., Soh, B.S., Lim, E., Reinhardt, F., Wu, Z.J., Krall, J.A., Bierie, B., Guo, W., et al. (2013). Protein kinase C α is a central signaling node and therapeutic target for breast cancer stem cells. Cancer Cell *24*, 347–364.

Tlsty, T.D., and Coussens, L.M. (2006). Tumor stroma and regulation of cancer development. Annu. Rev. Pathol. *1*, 119–150.

Tsukada, Y., Miyazawa, K., and Kitamura, N. (2001). High intensity ERK signal mediates hepatocyte growth factor-induced proliferation inhibition of the human hepatocellular carcinoma cell line HepG2. J. Biol. Chem. *276*, 40968–40976.

Vermeulen, L., De Sousa E Melo, F., van der Heijden, M., Cameron, K., de Jong, J.H., Borovski, T., Tuynman, J.B., Todaro, M., Merz, C., Rodermond, H., et al. (2010). Wnt activity defines colon cancer stem cells and is regulated by the microenvironment. Nat. Cell Biol. *12*, 468–476.

Xie, Q., Su, Y., Dykema, K., Johnson, J., Koeman, J., De Giorgi, V., Huang, A., Schlegel, R., Essenburg, C., Kang, L., et al. (2013). Overexpression of HGF promotes HBV-induced hepatocellular carcinoma progression and is an effective indicator for effective indicator. Genes Cancer *4*, 247–260.

Yamashita, T., Ji, J., Budhu, A., Forgues, M., Yang, W., Wang, H.Y., Jia, H., Ye, Q., Qin, L.X., Wauthier, E., et al. (2009). EpCAM-positive hepatocellular carcinoma cells are tumor-initiating cells with stem/progenitor cell features. Gastroenterology *136*, 1012–1024.

Yang, W., Yan, H.X., Chen, L., Liu, Q., He, Y.Q., Yu, L.X., Zhang, S.H., Huang, D.D., Tang, L., Kong, X.N., et al. (2008a). Wnt/beta-catenin signaling contributes to activation of normal and tumorigenic liver progenitor cells. Cancer Res. *68*, 4287–4295.

Yang, Z.F., Ho, D.W., Ng, M.N., Lau, C.K., Yu, W.C., Ngai, P., Chu, P.W., Lam, C.T., Poon, R.T., and Fan, S.T. (2008b). Significance of CD90+ cancer stem cells in human liver cancer. Cancer Cell *13*, 153–166.